

A HYBRID APPROACH TO PREDICT THE VIBRATION TRANSMISSION IN SHIP STRUCTURES USING A WAVEGUIDE METHOD AND STATISTICAL ENERGY ANALYSIS

Nicole J. Kessissoglou(1) and John Keir(2)

(1) School of Mechanical and Manufacturing Engineering, The University of New South Wales, Sydney 2052, Australia
(2) School of Engineering, James Cook University, Townsville QLD 4811, Australia

Abstract

Prediction of vibration transmission in ship structures is important, to design maritime vessels with greater power and reduced weight, without increasing noise levels. As the frequency increases, and hence the number of modes increases, it is more practical to consider average responses and their distribution over the structure, using a technique such as Statistical Energy Analysis (SEA). Numerical results from an exact, analytical waveguide model are compared with those of conventional SEA models. These results include both response predictions and the SEA parameters. The theoretical estimation of the SEA parameters, namely the coupling loss factors, form the basis for the hybrid approach between the waveguide method and SEA technique. Results are presented for plate structures in an L, T and X-shaped configuration, and a complex built-up structure.

Nomenclature

D	Flexural rigidity of the plate
h	Plate thickness
k	Wave number
ρ	Density
ω	Radian frequency

Introduction

A ship hull and bottom structure can act as an effective transmission path for structure-borne noise to locations at large distances from the source. In the low frequency range, where fewer modes excite the structure, deterministic methods such as analytical methods and finite element analysis are used to assess the vibrational response in connected plates [1]. As the frequency increases, and hence the number of vibrational modes increases, it is more practical to consider average responses and their distribution over the structure. Statistical energy analysis (SEA) is an energy balance method and considers the flow of energy into the system, the energy flow between subsystems, and the average energy contained within each subsystem [2,3]. The input powers and energies are time, space and frequency averaged, and a greater accuracy is achieved with a greater population of modes. SEA can provide no detail of the spatial distribution of the structural response, and there are a lot of effects of uncertainty and variability associated with SEA models. The successful use of SEA strongly depends on the accurate estimation of the three sets of SEA parameters corresponding to the modal densities, damping loss factors and coupling loss factors. Determination of these parameters, and in particular the coupling loss factors, is a central and difficult problem for SEA models [3]. The most common methods to determine the coupling loss factors are the wave

transmission approach [4,5] and finite element analysis [6].

In this paper, a simple well-known structure corresponding to an L-shaped plate is initially investigated. Energy levels of the coupled plates predicted from an exact analytical waveguide model are compared with those obtained from conventional SEA equations. A hybrid approach between the two techniques is presented. The hybrid method uses the analytical waveguide method to estimate the input power and coupling loss factors. The energy levels in a subsystem using the exact analytical method, SEA, and the hybrid technique are compared.

Analytical Waveguide Method

Consider a structure made up of two finite plates joined together at right angles along a common edge at $x_i = 0$ for $i = 1$ to 2, to form an L-shaped plate as shown in Figure 1. Both plates are simply supported along the edges $y = 0$ and $y = L_y$, and free at the other ends corresponding to $x_1 = L_{x1}$ and $x_2 = L_{x2}$. A point force is applied on plate 1 to generate flexural vibration, and is modelled by a Dirac delta function of force magnitude F_o at a location (x_o, y_o) .

The plate flexural displacement in the various sections can be described by:

$$w_i(x_i, y) = \sum_{m=1}^{\infty} \phi_m(x) \sin k_y y \quad (1)$$

$$\phi_m(x) = A_i e^{-jk_x x_i} + B_i e^{jk_x x_i} + C_i e^{-k_n x_i} + D_i e^{k_n x_i} \quad (2)$$

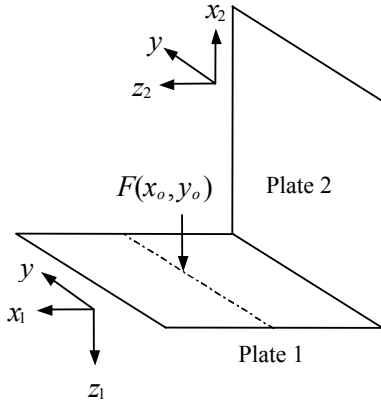


Figure 1. L-shaped plate under point force excitation.

where A_i and B_i are coefficients of the propagating waves, and C_i and D_i are coefficients of the near-field decay waves. $k_x = \sqrt{k_p^2 - k_y^2}$ is the propagating wave number in the x -direction, and $k_n = \sqrt{k_p^2 + k_y^2}$ is the wave number in the x -direction for the decay waves. $k_p = \sqrt{\omega(\rho h / D)^{1/4}}$ is the plate bending wave number. $k_y = m\pi / L_y$ is the wave number in the y -direction due to the simply supported boundary conditions, where $m = 1, 2, 3, \dots$ is the mode number. For plates of the same material properties, lengths and thicknesses, the various structural wave numbers are the same for each plate.

There are 12 unknown wave coefficients to be evaluated for the L-shaped plate. These can be found using boundary equations at the free edges, and the continuity equations at the driving force location and junction of the plates [7].

Statistical Energy Analysis

In an SEA model of an L-shaped plate as shown in Fig. 1, the plate can be separated into two physical systems corresponding to plate 1 and plate 2. The input power is injected to plate 1 only. The coupling of the SEA subsystems for bending vibration only is shown in Fig. 2. The power balance equations for the system are given in matrix form in Eq. (3).

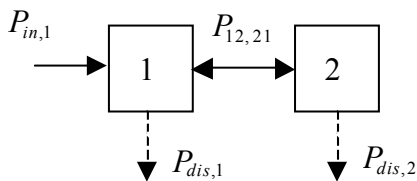


Figure 2. SEA power flow for the L-shaped plate.

$$\begin{Bmatrix} P_{in,1} \\ 0 \end{Bmatrix} = \omega \begin{bmatrix} \eta_1 + \eta_{12} & -\eta_{21} \\ -\eta_{12} & \eta_2 + \eta_{21} \end{bmatrix} \begin{Bmatrix} E_1 \\ E_2 \end{Bmatrix} \quad (3)$$

The energies in each plate, E_1 and E_2 can be determined by:

$$\begin{Bmatrix} E_1 \\ E_2 \end{Bmatrix} = \frac{1}{\omega} \begin{bmatrix} \eta_1 + \eta_{12} & -\eta_{21} \\ -\eta_{12} & \eta_2 + \eta_{21} \end{bmatrix}^{-1} \begin{Bmatrix} P_{in,1} \\ 0 \end{Bmatrix} \quad (4)$$

For coupling between multiple subsystems as in the case of T and X-shaped plates, the SEA power flow equation becomes [2-4]:

$$P_{in,i} = \omega \eta_i E_i + \sum_j \omega (\eta_{ij} E_i - \eta_{ji} E_j) \quad (5)$$

In conventional SEA models, the parameters of interest are the input power P_{in} , subsystem energies E , modal density n , internal loss factor η_i , and coupling loss factors η_{ij} .

Modal Density

The modal density $n(\omega)$ is defined as the number of vibrational modes per unit frequency, and is an important parameter in SEA. The modal density of a two-dimensional structure can be written as [2,8]:

$$n_{2-D} = \frac{\omega S}{2\pi c_g c} \quad (6)$$

where ω is the radian frequency, S is the area of the two-dimensional component, c_g is the group velocity, and c is the phase velocity ($c = \omega / k$). For bending vibration in thin plates, the phase velocity is:

$$c_p = \frac{\omega}{k_p} = \sqrt{\omega \left(\frac{D}{\rho h} \right)^{1/4}} \quad (7)$$

The group velocity is twice the phase velocity $c_g = 2c_p$. For a thin plate in bending vibration, Eq. (6) can be written as [8]:

$$n = \frac{L_x L_y}{4\pi} \sqrt{\frac{\rho h}{D}} \quad (8)$$

It can be seen in Eq. (8) that the modal density for bending vibration of thin plates becomes independent of the frequency.

Input Power

The input power is an important parameter in SEA calculations. If a point force F drives a system, then the total power supplied to the system is given by [4,8]:

$$P_{in} = \frac{F^2}{2} \operatorname{Re} \left(\frac{1}{Z} \right) \quad (9)$$

where Z represents the impedance of an infinite plate. When the power transmission into a plate (in bending vibration) is frequency averaged, it becomes independent of size, shape and boundary conditions, and proportional to the real part of the mobility of an infinite plate [8]. The mobility is equal to the inverse of the impedance. For a thin isotropic plate, the impedance Z is given by:

$$Z = 8\sqrt{D\rho} \quad (10)$$

Internal and Coupling Loss Factors

When materials are deformed, energy is absorbed and dissipated by the material. This is accounted for by using a structural (internal) loss factor η_i . The internal loss factor is dependent on frequency, but can be assumed constant when examining frequency ranges between 1 kHz and 10 kHz [3]. Internal loss factors for some common materials are given in Table 6.1 of reference 3.

The coupling loss factors are related to the transmission of vibrational energy between coupled subsystems in a built-up system. The coupling loss factor, η_{ij} , is the parameter used to determine the amount of ‘‘coupling’’ between two subsystems i and j . In SEA applications, it is desirable that the subsystems be weakly coupled, which occurs when the material loss factor is greater than the coupling loss factor, that is, $\eta_{ij} < \eta_i$ or

$\eta_{ij} < \eta_j$. For weakly coupled subsystems, energy is lost due to dissipation, and the structural loss factor dominates. For strongly coupled subsystems, energy is lost due to transmission, and hence the coupling loss factor dominates. Analytical expressions are available for coupling between structural elements such as line junctions between coupled plates and plate-cantilever beam junctions, as well as between structural and acoustic volumes [2-4,8]. The most widely used method to evaluate the coupling loss factors for systems connected along a line is to use the wave transmission approach [8]. Using the wave approach, the coupling loss factor η_{ij} is derived directly from the power transmission coefficient τ_{ij} , which is defined as the ratio of the transmitted to incident power at the boundary:

$$\tau_{ij} = \frac{\text{Transmitted power}}{\text{Incident power}} = \frac{P_{transmitted}}{P_{incident}} \quad (11)$$

When calculating the power transmission coefficient using the wave transmission method, the subsystems are assumed to be semi-infinite [2]. Therefore, waves impinging on the junction of two coupled subsystems i and j are reflected (in subsystem i) and transmitted (to subsystem j), but no reflection at the other boundaries of the subsystems away from the junction is taken into account. Equations (12) to (14) are the power transmission coefficients from plates 1 to 2 for the L, T and X-shaped plates respectively, in bending vibration only [8]. In deriving these expressions, it has been assumed that the group velocities in each plate are the same. All plates are the same material and σ is the plate thickness ratio. For plates of the same thickness ($\sigma = 1$), the power transmission coefficients for the L, T and X-shaped plates are given by the number on the right hand side in Eqs. (12) to (14) respectively.

$$\tau_{12} = 2(\sigma^{-5/4} + \sigma^{5/4})^{-2} = 0.5 \quad (12)$$

$$\tau_{12} = \left(\sqrt{2}\sigma^{-5/4} + \frac{\sigma^{5/4}}{\sqrt{2}} \right)^{-2} = 0.222 \quad (13)$$

$$\tau_{12} = 0.5(\sigma^{-5/4} + \sigma^{5/4})^{-2} = 0.125 \quad (14)$$

The general expression used to determine the coupling loss factor for two structures joined along a line in terms of the power transmission coefficient is given by [4,8]:

$$\eta_{ij} = \frac{2c_p L \langle \tau_{ij} \rangle}{\pi \omega S_i} \quad (15)$$

where L is the length of the junction line, ω is the centre frequency of the band of interest, and S_i is the surface area of the subsystem i . The brackets $\langle \rangle$ represent averaged over position, as the power transmission coefficient is averaged at all positions over the length of the junction.

The coupling loss factors satisfy the reciprocity relation of $n_i \eta_{ij} = n_j \eta_{ji}$ where n_i is the modal density of subsystem i . It was shown in Eq. (8) that the modal density for a thin plate in bending vibration is independent of the frequency, and is proportional to the surface area S of the plate. Hence, for two coupled plates of the same material parameters, the reciprocity relation can be written as $S_i \eta_{ij} = S_j \eta_{ji}$, where S_i and S_j are the surface areas of plates i and j respectively. Using the reciprocity relation, Eq. (5) can be written as:

$$P_{in,i} = \omega \eta_i E_i + \sum_j \omega \eta_{ij} S_i \left(\frac{E_i}{S_i} - \frac{E_j}{S_j} \right) \quad (16)$$

Hybrid Approach

The hybrid approach involves using the analytical waveguide model to estimate the input power and coupling loss factors used in the SEA equations. The hybrid method was initially developed for the L-shaped plate, and then extended to T and X-shaped plates, and finally the 7-plate structure shown in Fig. 3.

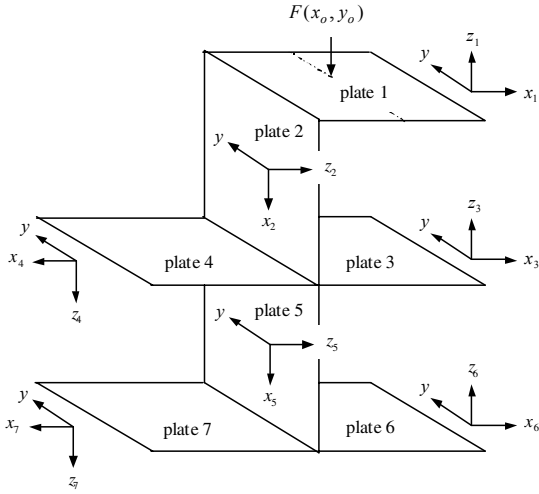


Figure 3. A built up 7-plate structure.

The input bending power for the SEA model was calculated by averaging the response over all possible excitation locations in the x - and y -directions. The time-averaged flexural input power at a given x -location is given by [9]:

$$\langle P_{in} \rangle = -\frac{1}{2} \text{Re} \left[(j\omega w)^* F_x - \left(j\omega \frac{\partial w}{\partial x} \right)^* M_x - \left(j\omega \frac{\partial w}{\partial y} \right)^* M_{xy} \right] \quad (17)$$

where the asterisk * denotes the complex conjugate, and the brackets represents average over position. F_x , M_x and M_{xy} are the bending shear force, bending moment and twisting moment respectively. The simply supported boundary conditions allowed the bending power to be averaged in the y -direction by integrating the power equation over the width of the plate from 0 to L_y . This results in a factor of 1/2 and removes the dependency of the input power on the y -location of the applied force. The input power was then averaged across the plate in the x -direction by driving the structure at a range of x -locations and then averaging the response. The

coupling loss factor η_{ij} was determined directly from the power transmission coefficient τ_{ij} and using the assumption of infinite plates. The assumption of the infinite boundary conditions was implemented by assuming no reflection from the free plate edges at $x_i = L_{x_i}$. For the L-shaped plate, the incident bending power was then found using the following expression for the propagating flexural displacement (in the negative x_1 direction) impinging at the coupling junction ($x_i = 0$):

$$w_1(x_1, y) = \sum_{m=1}^{\infty} B_1 \sin k_y y \quad (18)$$

Similarly, the transmitted bending power in plate 2 was found using the following expression for the transmitted propagating flexural waves at the coupling junction:

$$w_2(x_2, y) = \sum_{m=1}^{\infty} A_2 \sin k_y y \quad (19)$$

B_1 and A_2 are coefficients of propagating waves in plates 1 and 2 respectively. The power transmission coefficient was calculated by the ratio of the transmitted bending power to the incident bending power at the junction of the two plates found using Eqs. (17) and (11). The coupling loss factors were then calculated using Eq. (15). Once the input power and coupling loss factors were found using the analytical waveguide model, the energy levels of each plate were determined.

Results and Discussion

The plates were given material properties of aluminium with Young's modulus $E = 7.1 \times 10^{10} \text{ N/m}^2$, density $\rho = 2700 \text{ kg/m}^3$, Poisson's ratio of 0.3, and a structural loss factor of $\eta = 0.001$. The plate dimensions are $L_{x1} = L_{x2} = 0.6 \text{ m}$, $L_y = 0.5 \text{ m}$, and thickness $h = 2 \text{ mm}$. The energy levels of each plate found using the hybrid approach are compared with those obtained from the analytical waveguide method as well as using the conventional SEA equations. The hybrid results are averaged over every 100Hz frequency band, and the value presented at the centre frequency of each 100Hz band. Two frequency ranges were examined corresponding to up to 1 kHz (low to mid frequency range), and 5 to 6 kHz (mid to high frequency range). A sufficient number of modes were used in the computational modelling to accurately describe the response in the two frequency ranges of interest. This was achieved by ensuring that a sufficient number of modes were chosen in each frequency range such that all the results converged. The power transmission coefficients calculated from the hybrid method are also presented and compared with those given in Eqs. (12) to (14) from reference 8. The results presented are for bending motion only in the coupled

plates, although it could be expected that as the frequency increases, in-plane vibration will begin to have a significant role [9].

Figures 4 and 5 display the energy levels of plate 1 and plate 2 of the L-shaped structure respectively. The energy levels were found using the hybrid approach, the waveguide analytical method and SEA techniques for a frequency up to 1 kHz. The results indicate that the conventional SEA equations give a poor indication of the mean energy levels at low frequencies, and tends to over predict the energy levels by around 5 to 10 dB. It can be seen that the hybrid approach gives more accurate results over the entire frequency range. Comparing Figs. 4 and 5, there is a slight reduction of energy levels from plates 1 to 2 due to the energy lost through transmission at the structural joint.

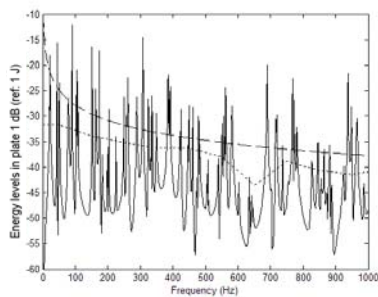


Figure 4. Energy levels in plate 1 of the L-shaped plate using the analytical waveguide method (solid line), SEA (dashed line), and the hybrid approach (dotted line).

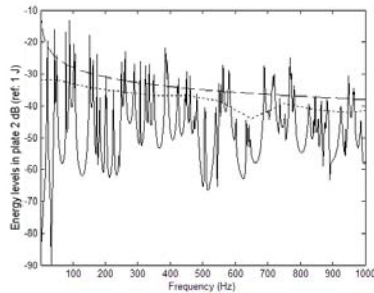


Figure 5. Energy levels in plate 2 of the L-shaped plate using the analytical waveguide method (solid line), SEA (dashed line), and the hybrid approach (dotted line).

The energy levels of plate 1 of the L-shaped plate calculated for a frequency range from 5 to 6 kHz is presented in Fig. 6. The results again show that in this frequency band, SEA over estimates the mean energy levels. In addition, using the conventional SEA equations, the mean energy levels become nearly a straight line due to a greater population of modes in this frequency range. It can also be observed that there is a dramatic decrease in the variance of the energy levels obtained using the analytical waveguide method as the frequency increases.

Figures 7 and 8 show a comparison of the power transmission coefficients τ_{12} calculated using the hybrid

approach with those predicted using Eq. (12), for the two frequency ranges. For a L-shaped structure, where the group velocities in each plate are the same, both plates are the same material, and the plate thickness ratio is unity, the transmission coefficient predicted by Eq. (12) is 0.5 and is a constant. In each case, it can be seen that the power transmission coefficient predicted using the hybrid method is slightly higher than the value presented in Eq. (12), although both values for τ_{12} are in very good agreement for all frequencies over the two frequency ranges.

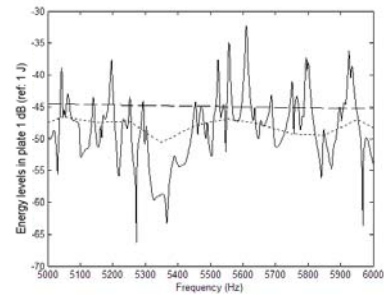


Figure 6. Energy levels in plate 1 of the L-shaped plate using the analytical waveguide method (solid line), SEA (dashed line), and the hybrid approach (dotted line).

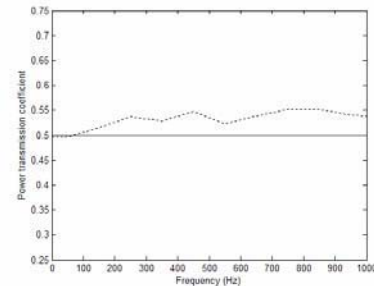


Figure 7. The power transmission coefficients τ_{12} for the L-shaped plate using the hybrid approach (dotted line), and predicted from Eq. (12) ($\tau_{12} = 0.5$) (solid line), for a frequency range from 1 Hz to 1 kHz.

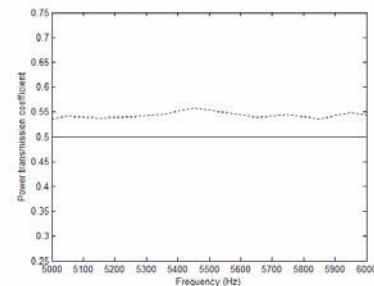


Figure 8. The power transmission coefficients τ_{12} for the L-shaped plate using the hybrid approach (dotted line), and predicted from Eq. (12) resulting in $\tau_{12} = 0.5$ (solid line), for a frequency range from 5 kHz to 6 kHz.

Very similar trends to the L-shaped plate were observed for the T and X-shaped plates, when comparing the energy levels obtained from the three methods. Figures 9 and 10 compare τ_{12} calculated from the hybrid approach and predicted from Eqs. (13) and (14) for the T and X-shaped plates respectively.

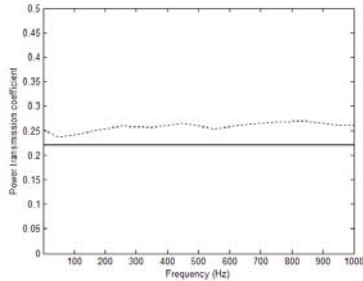


Figure 9. The power transmission coefficients τ_{12} for the T-shaped plate using the hybrid approach (dotted), and predicted from Eq. (13) ($\tau_{12} = 0.222$) (solid line).

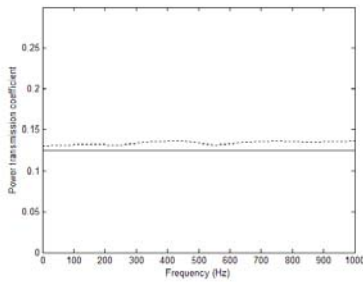


Figure 10. The power transmission coefficients τ_{12} for the X-shaped plate using the hybrid approach (dotted), and predicted from Eq. (14) ($\tau_{12} = 0.125$) (solid line).

Figures 11 and 12 present the energy levels of plate 2 of the 7-plate structure, for a frequency range up to 1 kHz, and from 5 to 6 kHz respectively. The SEA prediction gives a good approximation of the mean energy levels. The hybrid approach clearly follows the trend of the response from the analytical waveguide method, but appears to under predict the mean energy levels.

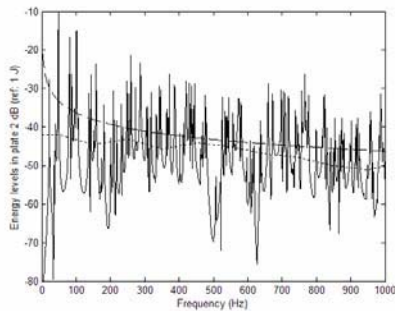


Figure 11. Energy levels in plate 2 of the 7-plate structure using the analytical waveguide method (solid), SEA (dashed line), and hybrid approach (dotted line).

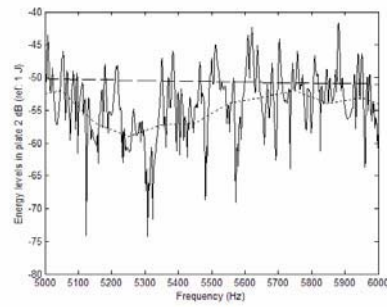


Figure 12. Energy levels in plate 2 of the 7-plate structure using the analytical waveguide method (solid), SEA (dashed line), and the hybrid approach (dotted line).

Conclusions

This paper presents preliminary results obtained from a hybrid approach in which the SEA parameters corresponding to the input power and coupling loss factors were obtained from an exact analytical waveguide method. Further work to validate the mean energy levels using conventional SEA equations can be performed in the higher frequency range with the inclusion of in-plane vibration.

References

- [1] P.G. Craven and B.M. Gibbs, "Sound transmission and mode coupling at junctions of thin plates, Part I: Representation of the problem", *Journal of Sound and Vibration*, 77: 417-427, 1981.
- [2] R.H. Lyon and R.G. DeJong, *Theory and application of statistical energy analysis*, Butterworth Heinemann, Oxford, 2nd ed., 1995.
- [3] M.P. Norton, *Fundamentals of noise and vibration analysis for engineers*, Cambridge University Press, Cambridge, 1989.
- [4] L. Cremer, M. Heckl and E.E. Ungar, *Structure-Borne Sound*. Springer-Verlag, 2nd ed. 1988.
- [5] R.S. Langley and K.H. Heron, "Elastic wave transmission through beam/plate junctions", *Journal of Sound and Vibration*, 143: 241-253, 1990.
- [6] C.R. Fredö, "SEA-like approach for the derivation of energy flow coefficients with a finite element model", *Journal of Sound and Vibration*, 199: 645-666, 1997.
- [7] J. Keir, N.J. Kessissoglou, and C.J. Norwood, "An analytical investigation of single actuator and error sensor control in connected plates", *Journal of Sound and Vibration*, 271: 635-649, 2004.
- [8] D.G. Crighton, A.P. Dowling, J.E. Ffowcs Williams, M. Heckl and F.G. Leppington, Chapter 8 in *Modern methods in analytical acoustics*, Springer-Verlag, London, 1992.
- [9] N.J. Kessissoglou, "Power transmission in L-shaped plates including flexural and in-plane vibration", *Journal of the Acoustical Society of America*, 115: 1157-1169, 2004.